

# DETERMINING THE CORRELATION BETWEEN SEAM ROUGHNESS AND VIBRATION IN FRICTION STIR WELDING

Ivo DRAGANOV, Svetlin STOYANOV, Danail GOSPODINOV, Nikolay FERDINANDOV, Yuliyan ANGELOV, Andrey DUNITSOV, Rossen RADEV

University of Ruse, Ruse, Bulgaria, EU, <u>iivanov@uni-ruse.bg</u>, <u>sstoyanov@uni-ruse.bg</u>, <u>dgospodinov@uni-ruse.bg</u>, <u>ruse.bg</u>, <u>nferdinandov@uni-ruse.bg</u>, <u>julian@uni-ruse.bg</u>

a.dunitsov@grema3d.com, rradev@uni-ruse.bg

https://doi.org/10.37904/metal.2025.5132

#### **Abstract**

The report presents the trial to correlation between roughness and vibration in friction stir welding of two aluminum plates. The transverse acceleration of the welded plates during welding was measured. The velocity and displacement in the transverse direction were determined by numerical integration. The welded joint was scanned and the profile in the joint area of the parts was obtained. The displacement results were compared with the roughness results. An analysis of the deviations in the two results was performed.

Keywords: Friction stir welding, vibration measurement, seam roughness, scanning

# 1. INTRODUCTION

Friction stir welding (FSW) is a process of joining solid bodies by mixing the materials around contact between them [1]. This process is carried out by the rotational movement of a third body, at a high temperature but below the melting point of the materials being welded. This technology is used for various types of aluminum alloys [2-7].

The vibrations occurring in the machines used in FSW are similar to the vibrations in metal-milling machines, which are the subject of intensive study [8]. The influence of vibrations in FSW has been established and studied by a number of authors. Fouladi et al. [5] studied the influence of vibrations on the corrosion resistance, mechanical properties and machining characteristics of the material. Balachandar et al. [4] considers the possibility of qualifying the welded joint using collected vibration data in the welding process. An artificial intelligence algorithm was used to evaluate the collected data and to perform an assessment of the welded joint.

Krishnamurthy et al. [3] measured the vibrations in the tool using a piezoelectric transducer. They obtained a time-amplitude diagram. Using the signal as input to support vector machine learning classifiers and determining the results of the tool to serve health and facilitate timely maintenance interventions.

Of particular interest is the FSW combined with ultrasonic vibrations. The introduction of high-frequency vibrations leads to an increase in plastic deformation in the material, a reduction in the gaps in the front part of the tool, and hence improved strength and toughness, which is described in [9]. For this purpose, evaluated tools are created [10].

Roughness and irregularities of the weld seam are the subject of study in the works [11, 12]. The measurement of roughness in these works was carried out with a surface roughness tester SJ-210. The work of Bhushan and Sharma [13] is also dedicated to the measurement of roughness. The advent of optical scanners allows the determination of the roughness of the resulting surfaces in a non-contact manner [14, 15].



The aim of this work is to find a correlation between vibrations in the welding process and the resulting roughness in the weld seam.

## 2. VIBRATION MEASUREMENT AND ROUGHNESS SCANNING IN FRICTION STIR WELDING

The FSW process was carried out on a universal milling machine FU 251. It is equipped with additional clamps that allows the workpieces to be welded to be pressed – **Figure 1**. The welded parts are two plates of aluminum 1050 with dimensions of 150x80x4 mm. To carry out the process, a tool made of quenched C45 steel with a shoulder diameter of 22 mm and a cylindrical pin with a normal M6 thread was used. The height of the pin is 3.6 mm.



Figure 1 Fixtures, weldments and sensors for vibration measurement

The welding process was performed at a speed of 315 mm/min at a spindle speed of 1000 rpm. The duration of the process was 33.68 sec. The length of the seam between the inlet and outlet holes of the tool was 176.8 mm. A Vernier triaxial acceleration sensor was used to measure the vibrations. The accelerometer has linear response up to 100 Hz, and this limits the minimal time step to 0.01 s. The sensor was attached to the welded plate using bolts and glue. The signal from the sensor was recorded on a laptop and processed using the LabVIEW program. The resulting welded joint was scanned with scanner Scantech KSCAN-Magic. The program ScanVewer was used to create an image of points saved in STL format. It was converted to STEP format using the QuickSurface software – **Figure 2**. The GOM2019 program was used for measurements.

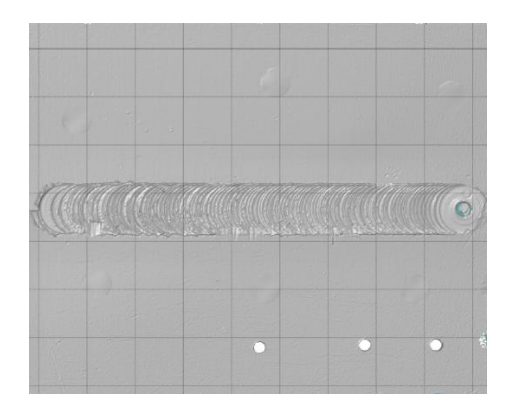


Figure 2 Three-dimensional scanned model of the welded joint

#### 3. VIBRATION MEASUREMENT RESULTS

The vibrations in the normal direction of the plane of the welded plates were measured. Results for the accelerations as a function of time were obtained – **Figure 3**, which are saved in a text file sensor.txt.



The results obtained for acceleration as a function of time in raw form were integrated over time and a velocity as a function of time diagram was obtained. The integration was performed according to the trapezoidal rule:

$$v(t) = \int a(t)dt \approx v_0 + \sum \frac{a_i + a_{i+1}}{2} \Delta t \tag{1}$$

where:

v(t) - the velocity as a function of time (m/s)

a(t) - the acceleration as a function of time (m/s<sup>2</sup>)

 $v_0$  - the initial velocity (m/s)

 $a_i$  and  $a_{i+1}$  - the accelerations in steps i and i+1 accordingly (m/s<sup>2</sup>)

 $\Delta t$  - the time step, (s)

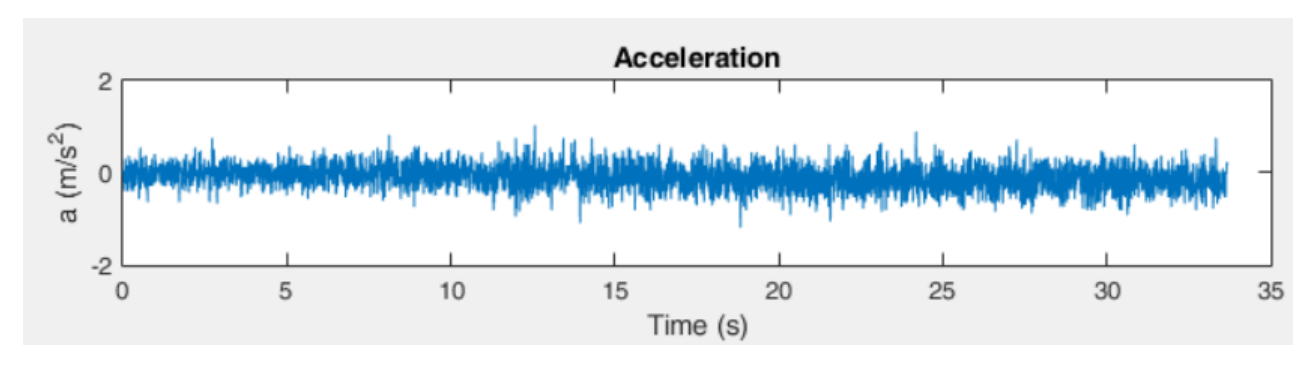


Figure 3 Raw time diagram of acceleration in the transverse direction

A script file was created in Matlab named vibscan.m. It is used to perform calculations and visualization. The results are highly dependent on the initial conditions and the noise present in the raw measurement data, which causes velocity drift. To overcome this problem, several filters were applied sequentially. First, the average value was subtracted from the raw acceleration signal. Then, the Savitzky-Golay filter [16] and the high-pass filter [17] were applied sequentially. The results of these transformations are given in **Figure 4**.

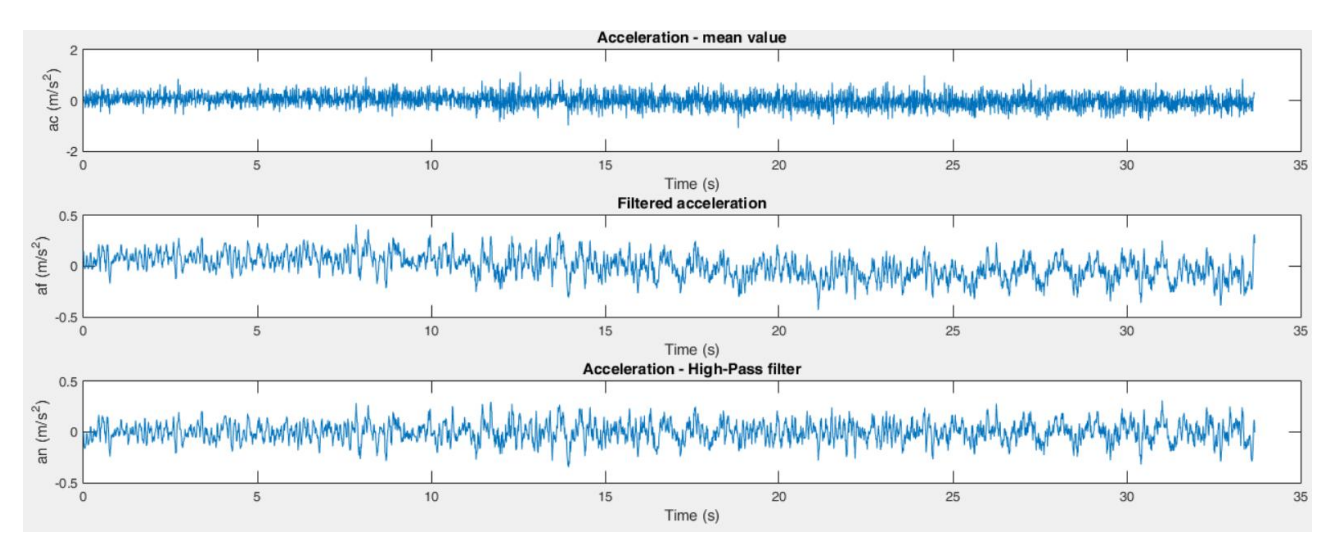


Figure 4 Mean value filter, Savitzky-Golay filter, high-pass filter

The obtained acceleration diagrams as a function of time were integrated according to formula (1) and the results for the velocity were obtained – **Figure 5**. The initial velocity was taken as the average velocity for the process, which was calculated to be  $v_0 = 0.021015$  m/s. This value minimizes the drift.



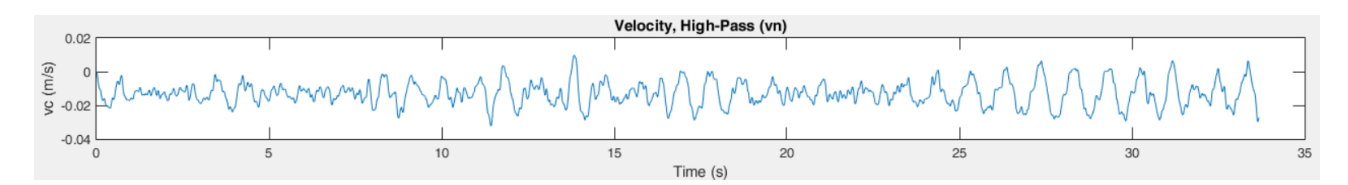


Figure 5 Velocity after applying the filters for the acceleration

To obtain the displacement function, the velocity function is integrated using the trapezoidal rule:

$$z_i = \int v(t)dt \approx +\sum z_{i-1} + \frac{v_i + v_{i-1}}{2} \Delta t$$
 (2)

where:

 $z_i$  - the displacement in normal direction to the plates as a function of time (m)

a(t) - the velocity as a function of time (m/s)

 $z_{i-1}$ - the displacement in the previous step (m)

 $v_i$  and  $v_{i-1}$  - the velocities in steps i and i-1 accordingly (m/s)

 $\Delta t$  - the time step, (s)

The displacement is obtained, and the drift is also observed in it. This also requires the removal of the average velocity and the best straight-fit line from the data from the velocity function. Then, for the displacement function, the diagrams in **(Figure 6)** and are obtained, respectively.

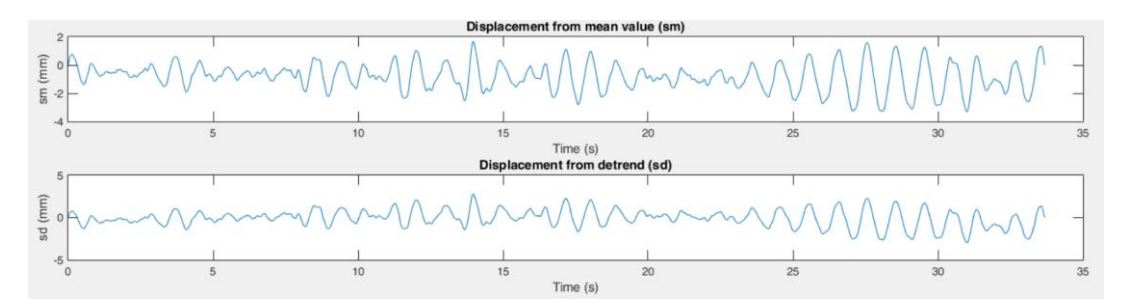


Figure 6 Displacement after removing the mean velocity and detrending from the velocity

## 4. ROUGHNESS MEASUREMENT RESULTS

Scanning the plate provides information about the roughness of the plate in the weld seam. The resulting three-dimensional model is cut along the section between the two plates and the values are measured relative to a line formed by the lower plane of the welded joint and the plane of contact between the plates – **Figure 7**.

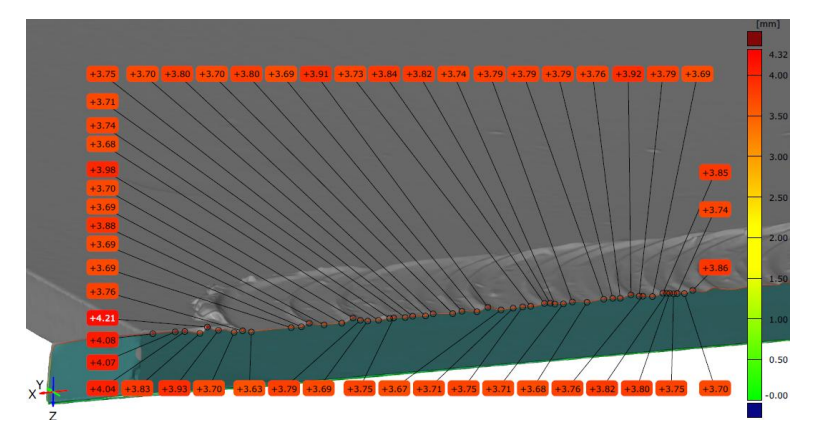


Figure 7 Determining weld roughness from scanned image



The numerical values for the roughness are saved in the file scener.txt. In the script file vibscan.m, the roughness is recalculated relative to a midline, so that the roughness is evenly distributed on the upper and lower sides of this line. A recalculation is also performed, as the displacements are converted from a function of coordinates into a function of time. The result of this is presented in **Figure 8**.

Edge effects associated with large shape changes, including those related to the instrument exit hole, have been removed from the roughness file. It is assumed that coordinates with a height greater than 3.8 mm relative to the baseline, which are located at both ends of the plate, will not be included in the analysis.

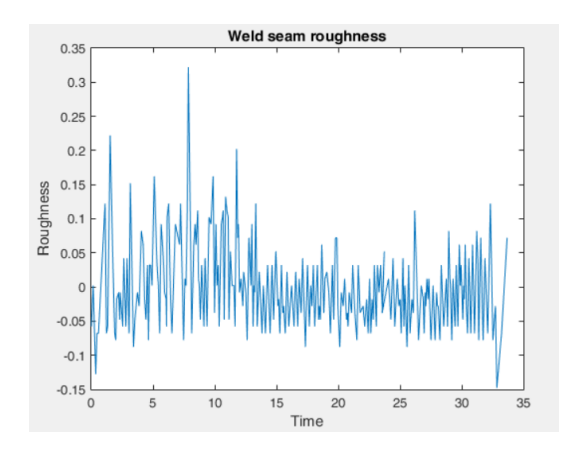


Figure 8 Weld roughness, recalculated as a function of time

## 5. COMPARISON AND ANALYSIS OF RESULTS

The results obtained for the displacements by double integration of the accelerations differ significantly from the results for the roughness. The maximum amplitude of the displacements is  $2.9813 \, \text{mm}$ , while the maximum roughness is  $0.32216 \, \text{mm}$ . A cross-correlation calculation was performed – **Figure 9**, which shows that Maximum correlation is achieved at lag =  $-3242 \, \text{samples}$ .

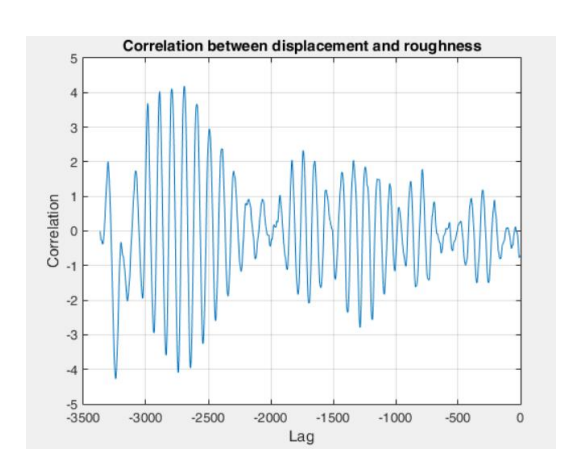


Figure 9 Cross-correlation

#### 6. CONCLUSION

The integration of the collected acceleration signal gives large deviations for the displacement. No clear correlation between vibrations and weld roughness has been found. It has been found that the initial conditions during integration have a large influence on the final result.



The studies should be continued for a shorter weld. Particular attention should be paid to the initial conditions and the edge effects. It is advisable to perform numerical simulations to determine whether a better correlation between the acceleration data and the roughness is possible.

## **ACKNOWLEDGEMENTS**

This study is financed by the European Union-NextGenerationEU, through the National Recovery and Resilience Plan of the Republic of Bulgaria, project № BG-RRP-2.013-0001.

## **REFERENCES**

- [1] THOMAS, W., NICHOLAS, E., NEEDHAM, J., CHURCH, M., TEMPLESMITH, P. International Patent Application No. PCT/GB92/002203 and GB Patent Application No. 9125978.9, 1991.
- [2] PATSALIAS, G.; SOFIAS, K.; VAIRIS, A. Solid-State Welding of Thin Aluminum Sheets: A Case Study of Friction Stir Welding Alloys 1050 and 5754. *Metals* 2025, vol. 15, 463. <a href="https://doi.org/10.3390/met15040463">https://doi.org/10.3390/met15040463</a>
- [3] KRISHNAMURTHY, B., RAKKIYANNAN, J., GNANASEKARAN, S., THANGAMUTHU, M. Condition monitoring of friction stir welding tool with vibration signals using support vector machine classifiers. *Engineering Research Express* 7, 2025, vol. 1, 015564. <a href="https://doi.org/10.1088/2631-8695/adb93b">https://doi.org/10.1088/2631-8695/adb93b</a>
- [4] BALACHANDAR, K., JEGADEESHWARAN, R., GANDHIKUMAR, D., Condition monitoring of FSW tool using vibration analysis A machine learning approach. *Materials Today: Proceedings*, 2020, vol. 27, Part 3, pp. 2970-2974. https://doi.org/10.1016/j.matpr.2020.04.903
- [5] FOULADI, S., GHASEMI, A.H., ABBASI, M., ABEDINI, M., KHORASANI, A.M., GIBSON, I. The Effect of Vibration during Friction Stir Welding on Corrosion Behavior, Mechanical Properties, and Machining Characteristics of Stir Zone. *Metals*, 2017, vol. 7, pp. 421. <a href="https://doi.org/10.3390/met7100421">https://doi.org/10.3390/met7100421</a>
- [6] WU, C., WANG, J., WANG, Q., XIA, P., LI, D. 7075 aluminum alloy Friction Stir Welding (FSW): Quality analysis and mechanical properties with WC-Co tool, *Materials Today Communications*, 2024, vol. 38, 108203. <a href="https://doi.org/10.1016/j.mtcomm.2024.108203">https://doi.org/10.1016/j.mtcomm.2024.108203</a>
- [7] LAKSHMI, A. A., CHALLA, B., SATEESH, N., DURGA RAJESH, K. V., REVATHI, G., VAFAEVA, K. M., & JOSHI, A. Friction stir welding of aluminum AA6061 & AA8011 using optimization approach based on both Taguchi and grey relational analysis. *Cogent Engineering*, 2024, vol. 11(1). https://doi.org/10.1080/23311916.2024.2393737
- [8] DIMITROV, D. Investigation of the Influence of Technological Parameters on Vibration Resistance in Modeling the Technological System. *Proceeding of University of Ruse*, Ruse, 2021, pp. 38-45.
- [9] DING, W, WU, C. Effect of ultrasonic vibration exerted at the tool on friction stir welding process and joint quality, *Journal of Manufacturing Processes*, 2019, vol. 42, pp. 192-201. https://doi.org/10.1016/j.jmapro.2019.04.026
- [10] AMINI, S., NAZARI, M.M., REZAEI, A. Bending vibrational tool for friction stir welding process. *The International Journal of Advanced Manufacturing Technology*, 2016, vol. 84, pp. 1889–1896.
- [11] GAIKWAD V., CHINCHANIKAR, S. Investigation on surface roughness, ultimate tensile strength, and microhardness of friction stir welded AA7075-T651 joint, *Materials Today: Proceedings*, 2021, vol. 46, Part 17. Pp. 8061-8065. <a href="https://doi.org/10.1016/j.matpr.2021.03.034">https://doi.org/10.1016/j.matpr.2021.03.034</a>
- [12] IKUMAPAYI O., AKINLABI, E. Experimental data on surface roughness and force feedback analysis in friction stir processed AA7075 – T651 aluminium metal composites, *Data in Brief*, 2019, vol. 23, 103710. https://doi.org/10.1016/j.dib.2019.103710
- [13] BHUSHAN, R.K., SHARMA, D. Investigation of mechanical properties and surface roughness of friction stir welded AA6061-T651. *Int J Mech Mater Eng*, 2020, vol. 15, 7. <a href="https://doi.org/10.1186/s40712-020-00119-x">https://doi.org/10.1186/s40712-020-00119-x</a>
- [14] BIZJAK, K., Determining the surface roughness coefficient by 3D Scanner, Geologija, 2010, vol. 53/2.
- [15] THORNBUSH, M. Measuring Surface Roughness through the Use of Digital Photography and Image Processing. International Journal of Geosciences, 2014, vol. 5, pp. 540-554. doi: 10.4236/ijg.2014.55050
- [16] ORFANIDIS, S. Introduction to Signal Processing. Englewood Cliffs, NJ: Prentice Hall, 1996.
- [17] BUI, N., BYUN, G. The Comparison Features of ECG Signal with Different Sampling Frequencies and Filter Methods for Real-Time Measurement. *Symmetry*, 2021, vol. 13, 1461. <a href="https://doi.org/10.3390/sym13081461">https://doi.org/10.3390/sym13081461</a>